Journal of Microscopy

Journal of Microscopy, Vol. 263, Issue 2 2016, pp. 171–180 doi: 10.1111/jmi.12395
Received 3 December 2015; accepted 10 February 2016

Interaction between the moss *Physcomitrella patens* and *Phytophthora*: a novel pathosystem for live-cell imaging of subcellular defence

ELYSA J. R. OVERDIJK*,†, JEROEN DE KEIJZER†, DEBORAH DE GROOT*, CHARIKLEIA SCHOINA*, KLAAS BOUWMEESTER*,‡, TIJS KETELAAR† & FRANCINE GOVERS*

**Laboratory of Phytopathology, Wageningen University, Wageningen, The Netherlands*

†Laboratory of Cell Biology, Wageningen University, Wageningen, The Netherlands

‡Plant-Microbe Interactions, Utrecht University, Utrecht, The Netherlands

Key words. Live-cell imaging, *Phytophthora capsici*, *Phytophthora infestans*, *Physcomitrella patens*, plant–pathogen interaction, subcellular defence.

Summary

Live-cell imaging of plant–pathogen interactions is often hampered by the tissue complexity and multicell layered nature of the host. Here, we established a novel pathosystem with the moss *Physcomitrella patens* as host for *Phytophthora*. The tip-growing protonema cells of this moss are ideal for visualizing interactions with the pathogen over time using high-resolution microscopy. We tested four *Phytophthora* species for their ability to infect *P. patens* and showed that *P. sojae* and *P. palmivora* were only rarely capable to infect *P. patens*. In contrast, *P. infestans* and *P. capsici* frequently and successfully penetrated moss protonemal cells, showed intracellular hyphal growth and formed sporangia. Next to these successful invasions, many penetration attempts failed. Here the pathogen was blocked by a barrier of cell wall material deposited in papilla-like structures, a defence response that is common in higher plants. Another common response is the upregulation of defence-related genes upon infection and also in moss we observed this upregulation in tissues infected with *Phytophthora*. For more advanced analyses of the novel pathosystem we developed a special set-up that allowed live-cell imaging of subcellular defence processes by high-resolution microscopy. With this set-up, we revealed that *Phytophthora* infection of moss induces repositioning of the nucleus, accumulation of cytoplasm and rearrangement of the actin cytoskeleton, but not of microtubules.

Introduction

Plant pathogens cause enormous crop losses worldwide and are often difficult to control. For designing novel control strategies, we need to gain more in depth knowledge on molecular and subcellular plant defence processes. Upon pathogen recognition, plant cells initiate a dramatic reprogramming to prevent penetration. This results, for example, in the production of antimicrobial compounds, movement of organelles, reinforcement of cell walls or rearrangement of the cytoskeleton (Schmelzer, 2002; Robatzek, 2007; Hardham, 2007). Over the last decades, advanced methods for imaging cell biological processes have been developed and were used to visualize subcellular rearrangements upon infection of plants by biotrophic fungi and oomycetes (Schmelzer, 2002; Hardham, 2007; Huckelhoven & Panstruga, 2011; Ben Khaled *et al.*, 2015). Often these studies make use of fixed plant tissue which has as major drawback that the dynamics of the plant–pathogen interaction cannot be captured. Preferably, live-cell imaging is used, but here the drawback is the multicell layered nature of the host that hampers high-resolution microscopy. Unlike higher plants, the moss *Physcomitrella patens* is ideal for high-resolution microscopy. Because this moss is also known to be susceptible to a variety of pathogens, we set out to further exploit *P. patens* as a model host plant. In this study, we first tested the ability of the oomycete pathogen *Phytophthora* to infect *P. patens* and subsequently developed a live-cell imaging set-up to investigate the host-pathogen interactions at the subcellular level.

The genus *Phytophthora* belongs to the class of oomycetes and comprises over 130 species that are all pathogens on a wide variety of plants (Kroon *et al.*, 2012). Notorious species are *Phytophthora infestans*, the causal agent of potato and tomato late blight (Fry, 2008) and *Phytophthora sojae*, the causal agent of stem rot and root rot in soybean. Examples of broad host range species are *Phytophthora capsici* that infects amongst others tomato and pepper (Lamour *et al.*, 2012) and *P. palmivora* that is pathogenic on tropical crops such as

Correspondence to: Francine Govers, Laboratory of Phytopathology, Wageningen University, Droevendaalsesteeg 16708 PB Wageningen, The Netherlands. Tel: +31 317 483 138; e-mail: francine.govers@wur.nl

© 2016 The Authors
Journal of Microscopy © 2016 Royal Microscopical Society

cacao and date palm. For asexual reproduction, *Phytophthora* produces sporangia that can either germinate directly or develop into zoosporangia. The latter releases motile zoospores that encyst upon touching a surface and then germinate. At the germ tube tip an appressorium is formed that enables host cell penetration. In higher plants the mycelium grows in between the mesophyl cells and forms feeding structures called haustoria that invade the cells. When the lesion expands, sporangiophores emerge through the stomata and the sporangia that are formed can start a new infection cycle (Hardham, 2001; Judelson & Blanco, 2005).

P. patens is a leafy bryophyte growing in many temperate regions worldwide. The bryophytes diverged around 450 million years ago from a common ancestor shared with vascular plants and thus form an evolutionary link between green algae and vascular plants (Knight *et al.*, 2009). During its lifecycle, *P. patens* is largely haploid with only a very short diploid, sporophytic phase. Upon germination, the haploid spores form a filamentous network called protonema and this protonema differentiates into gametophores with small leaf-like phyllidia and rhizoids. After fertilization a diploid sporophyte develops on top of these gametophores that undergoes meiosis to produce the next generation of haploid spores (Cove, 2005). *P. patens* has become an important model system for functional genomics and cell biology. It is easily cultured and its highly efficient homologous recombination allows direct gene targeting (Nishiyama *et al.*, 2000). Moreover, the fact that protonema and phyllidia are one-cell-layer-thick, makes *P. patens* ideal for microscopy.

In nature, mosses are infected by microbial pathogens often leading to severe damage (Davey & Currah, 2006; Davey *et al.*, 2009). To exploit the advantages of *P. patens* as a model host plant, several pathogens have been tested for their ability to infect *P. patens*. For the fungal pathogens *Botrytis cinerea, Altenaria brassicicola, Altenaria alternata, Fusarium avenaceum* and *Fusarium oxysporum* (Ponce de Léon *et al.*, 2007; Akita *et al.*, 2011; Bressendorff, 2012; Lehtonen *et al.*, 2012b; Ponce de Léon *et al.*, 2012), the bacterium *Pectobacterium carotovorum* (Andersson *et al.*, 2005; Ponce de Léon et al., 2007) and three species of the oomycete genus *Pythium* (Oliver et al., 2009; Takikawa *et al.*, 2015), it has been shown that they are capable to infect *P. patens*. More recently, Reboledo *et al.* (2015) described the infection of *P. patens* by the hemibiotrophic pathogen, *Colletotrichum gloeosporioides*. These studies revealed that these pathogens cause extensive cell death of moss tissue and induce defence responses in *P. patens* that are similar to those activated in flowering plants (Ponce de León, 2011; Ponce de León & Montesano, 2013). For example, inoculation with the *Pythium* species, *B. cinerea* and *C. gloesporioides* resulted in cell wall reinforcement and the production of reactive oxygen species (ROS) (Oliver et al., 2009; Ponce de Léon et al., 2012; Reboledo *et al.*, 2015) and exposing *P. patens* tissue to the fungal elicitors chitin and chitosan lead to a rapid ROS burst, increased peroxidase activity and induction of chitinase secretion (Lehtonen *et al.*, 2009; Lehtonen *et al.*, 2012a; Lehtonen *et al.*, 2014). Furthermore, levels of the hormone salicylic acid (SA) and a precursor of jasmonic acid (JA) were found to be increased upon *B. cinerea* infection (Ponce de Léon et al., 2012). Also, several genes encoding defence-related proteins were found to be upregulated upon pathogen attack or elicitor treatment (Oliver et al., 2009; Bressendorff, 2012; Ponce de Léon et al., 2012; Lehtonen et al., 2012a; Reboledo et al., 2015). These included genes encoding phenylalanine ammonia lyase (PAL) and chalcone synthase (CHS), both enzymes in the flavonoid pathway that produces antimicrobial compounds and is involved in SA accumulation (Huang *et al.*, 2010; Dao *et al.*, 2011), and a lipoxygenase (LOX) that is part of the oxylipin pathway of which JA is one of the products (Porta & Rocha-Sosa, 2002). Also genes encoding the superoxide producer NADPH oxidase (NOX), (Sagi & Fluhr, 2006), the mitogen activated protein kinase 4a (MPK4A) that in Arabidopsis is involved in early defence signalling (Berriri *et al.*, 2012), and the transcription factor ethylene-responsive element-binding factor 5 (ERF5) were upregulated. Together, these findings indicate that basal defence signalling was already present prior to the emergence of higher plants. Once penetration in higher plants has been achieved, the pathogen can still be stopped by a local hypersensitive response (HR) which is triggered by resistance proteins that recognize pathogen effectors (van Ooijen *et al.*, 2007). The genome of *P. patens* contains several resistance gene homologs (Akita & Valkonen, 2002; Xue *et al.*, 2012; Tanigaki *et al.*, 2014), but as yet activation of HR in moss has not been reported.

In this study, we describe a novel pathosystem with *P. patens* as host for two *Phytophthora* species. We characterized the infection of *P. patens* by *P. infestans* and *P. capsici* and analysed defence responses upon attack by these pathogens, including cell wall fortification and the induction of defence-related gene expression. We also demonstrate the high potential of this pathosystem for high-resolution live-cell imaging of subcellular defence by visualizing local reorganisation of the actin cytoskeleton in *P. patens* upon *Phytophthora* infection.

Material and methods

P. patens *culturing conditions*

P. patens wild-type isolate Gransden (Ashton & Cove, 1977) was routinely cultured on BCDAT or BCD agar (Nishiyama *et al.*, 2000) at 25°C under continuous white light.

Transformation of P. patens

To create a moss line in which both actin filaments and microtubules are fluorescently labelled, a LifeAct-eGFP construct (Vidali *et al.*, 2009) was transformed into a moss line expressing a gene encoding mCherry fused to α-tubulin driven by

© 2016 The Authors

the rice actin promoter (McElroy *et al.*, 1990) and integrated at the HB7 locus (Hiwatashi *et al.*, 2008) (T. Miki, unpublished). Transformation was performed using PEG-mediated protoplast transfection (Nishiyama *et al.*, 2000) and stable transformants were selected by resistance to hygromycin after a period of release from selection.

Pathogen growth conditions and inoculum preparation

Isolates of *P. capsici*, *P. palmivora* and *P. sojae* (Table 1) were cultured on 20% (v/v) V8 juice agar at 25°C under continuous light (Erwin & Ribeiro, 1996). *P. infestans* was cultured on rye sucrose agar at 18°C in the dark (Caten & Jinks, 1967). To produce inoculum, 11–14-day-old colonies of *P. infestans* were flooded with sterilized cold water, followed by incubation at 4°C for 3 h in the dark. Zoospores of *P. palmivora* were obtained by flooding 5–7-day-old colonies with sterilized cold water, followed by 30-min incubation at 25°C in light. A similar method was used to isolate zoospores of *P. capsici*, with the difference that plates were unsealed and grown under continuous light to produce sporangia. Zoospores were filtered through a 0.5-μm filter, concentrations were measured using a haemocytometer and adjusted to 1×10^5 to 1×10^6 zoospores mL^{-1}. Inoculation with *P. sojae* was done with mycelial plugs of 0.3 cm in diameter from the edge of a 5-day-old colony.

Trypan blue staining

P. patens was grown on BCD agar overlaid with cellophane for 2–3 weeks and inoculated with a 50 μL droplet of inoculum containing 1×10^5 zoospores mL^{-1} per colony. Inoculated moss tissue was stained in trypan blue solution (10 mL phenol, 10 mL glycerol, 10 mL lactic acid, 10 mL water, 0.02 g trypan blue) overnight and destained with chloral hydrate for at least 1 day (Wilson & Coffey, 1980).

P. patens *growth and inoculation for live-cell imaging of infected cells*

Protonemal tissue was grown in a glass-bottom microwell dish of 35 mm in diameter (MatTek, Ashland, USA). This dish was first filled with BCD 1,2% agar (w/v), subsequently a 1 cm $\times$ 1 cm agar square was removed from the coverglass of the dish and a small moss explant was placed on the bottom. This explant was covered by a 1-mm thin layer of BCD 0.7% low melting point agar (w/v) and protonemal tissue was grown under standard conditions for 5–7 days prior to inoculation. Subsequently, a 20-μL droplet of inoculum containing in total 1×10^6 zoospores mL^{-1} was placed on top of the protonemal tissue. Inoculated dishes were sealed with surgical micropore tape (3M Health Care Business, Neuss, Germany) and placed at the bench at room temperature for at least 4 h before microscopic observation.

Microscopy

Brightfield microscopy was performed on a Nikon 90i microscope (Nikon, Amstelveen, The Netherlands) using differential interference contrast and a 60$\times$ water immersion 1.20 NA objective. Confocal fluorescence microscopy was performed using a Roper Spinning Disc Confocal Microscope (Nikon Ti microscope body, Yokogawa CSUX1-spinning disc head, Photometrics Evolve camera, Metamorph software, 491 and 561 nm laser lines; GFP filter 495–560 nm; mCherry filter 570–620 nm; 100$\times$ oil immersion 1.40 NA objective; 1.2$\times$ magnification lens between spinning disk head and camera). Z-stacks were acquired with an internal Z-spacing of 0.5 μm and image processing was performed using ImageJ software.

Quantitative RT-PCR

P. patens protonemal tissue was homogenized with a polytron homogenizer, plated on BCDAT agar overlaid with cellophane and grown for 1 week. Subsequently, moss plates were sprayed with in total 1 mL of 1×10^6 zoospores mL^{-1} per 9-cm plate. Inoculated moss plates were sealed with surgical micropore tape (3M Health Care Business) and placed at 25°C under continuous light. Mock inoculations were performed using sterilized deionized water. Total RNA was isolated from infected and mock-treated moss tissue by a Quick-RNA MiniPrep kit (Zymo Research, CA, USA). Synthesis of cDNA was performed on 2 μg of total RNA using a M-MLV reverse transcriptase kit (Promega, Madison, WI, USA). qRT-PCR was performed in a Bio-Rad 7300 Real Time PCR system (Applied Biosystems, NY, USA) and using a SYBR Hi-ROX kit (Bioline, London, UK), gene-specific primers (Table 2) and 3 μL of 10-times diluted cDNA. Gene expression levels were normalized to EF1α transcript levels and to the transcript levels of the studied gene in mock-inoculated moss tissue.

Results and discussion

P. infestans *and* P. capsici *are able to infect* P. patens

As a first step, we tested four *Phytophthora* species for their ability to infect *P. patens*. Moss colonies were inoculated with zoospores of *P. infestans, P. capsici, P. palmivora* and *P. sojae* and stained with trypan blue to visualize mycelium or spores of the pathogen and dead or damaged cells of the moss.

Inoculation with *P. sojae* rarely resulted in infection of *P. patens*. Only occasionally we observed local cell death reminiscent of successful colonization. Sometimes we also found oospores (i.e. sexual spores) inside cells of phyllidia and on protonemal tissue demonstrating that *P. sojae* is capable to grow and expand in moss (Fig. 1A). *P. sojae* is homothallic and during interaction with its natural host soybean it readily produces oospores inside infected tissues (Erwin & Ribeiro, 1996). Also *P. palmivora* was hardly able to infect moss cells (Fig. 1B).

© 2016 The Authors

Table 1. *Phytophthora* isolates used in this study

Phytophthora species	Isolate	Origin	Refrence
P. infestans	14-3-GFP	*GFP*-expressing transformant of *P. infestans* H30P02	–
P. capsici	LT263	Isolated from pumpkin	(Donahoo & Lamour, 2008)
	LT3239	Isolated from pumpkin	–
P. sojae	P6497	Isolated from soybean	(Forster *et al.*, 1994)
P. palmivora	GFP3	*GFP*-expressing transformant of *P. palmivora* P6390	(Vijn & Govers, 2003)

Table 2. Primers used in this study

Gene	Gene ID[a]	Forward (Fw) and reverse (Rv) primer	Reference
PpPAL4	Pp1s500_4V6.1	Fw: TGGCCTACTCGGTAATGGAG Rv: GTCAACCATCCGCTTGATTT	(Bressendorff, 2012)
PpLOX7	Pp1s70_182V6.1	Fw: GTGGCGGTTTGATCAGGA Rv: CGTTCAGCCATCCCTCTTC	(Lehtonen *et al.*, 2012a)
PpNOX	Pp1s18_194V6.1	Fw: CACGATGTTGCAGTCGTTG Rv: TACGTGCCCTAGTGCCTGA	(Lehtonen *et al.*, 2012a)
PpCHS	Pp1s22_4V6.1	Fw: GGCATGGAACGAGATGTTCT Rv: CCTTGCATCTTGTCCTTGGT	(Bressendorff, 2012)
PpERF5	Pp1s2_410V6.1	Fw: GCTCCGCTGTATCGAAAGTC Rv: TCGAAGTTGCTGACAAGGTG	(Bressendorff, 2012)
PpMPK4A	Pp1s149_39V6.1	Fw: GGTACAAGCCACCACTTCGT Rv: GGTCCGTATCCATCAACTCG	(Bressendorff, 2012)
PpEF1a	Pp1s163_112V6.2	Fw: AATCATACATTTCACCTCGCC Rv: GATCAGTGGGTAGAAGTGAC	(Le Bail *et al.*, 2013)

[a]Gene IDs used by www.cosmoss.org.

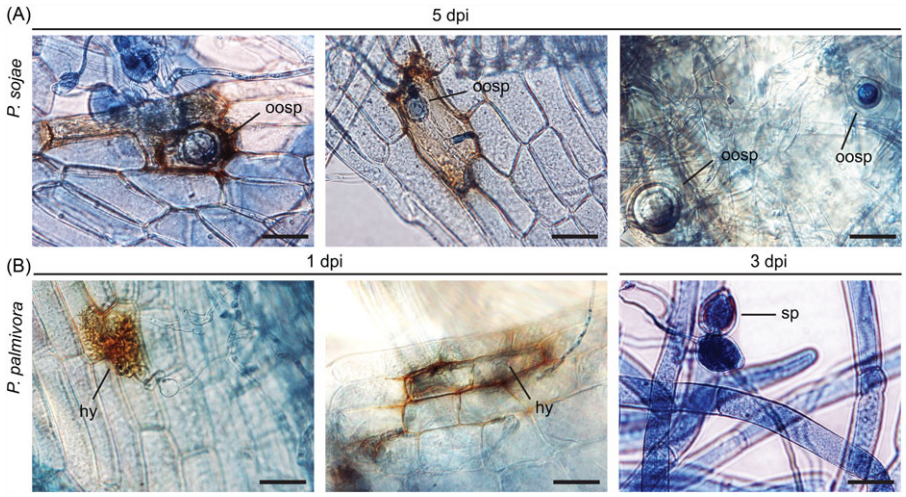

Fig. 1. *P. sojae* and *P. palmivora* occasionally infect *P. patens*. *P. patens* at 5 days postinoculation (dpi) with *P. sojae* (A) and at 1 and 3 dpi with *P. palmivora* (B). The tissue was stained with trypan blue and visualised by brightfield microscopy. Scale bars represent 20 μm. hy, intracellular hypha; oosp, oospore; sp, sporangium.

Local cell death, cell wall browning and intracellular hyphal growth were observed in gametophore phyllidia cells. At a later stage of infection, that is, 3 days postinoculation (dpi), sporangia were formed on moss tissue. Because infection by either *P. sojae* or *P. palmivora* was rarely observed, these two species were not used for further study.

Inoculation with the other two *Phytophthora* species did result in more frequent infections and browning of moss tissue, indicating that *P. patens* is susceptible to these pathogens (Fig. 2A). Upon inoculation with both *P. infestans* and *P. capsici*, appressoria were formed that enabled penetration of moss cells and we observed hyphae growing inside these cells

© 2016 The Authors

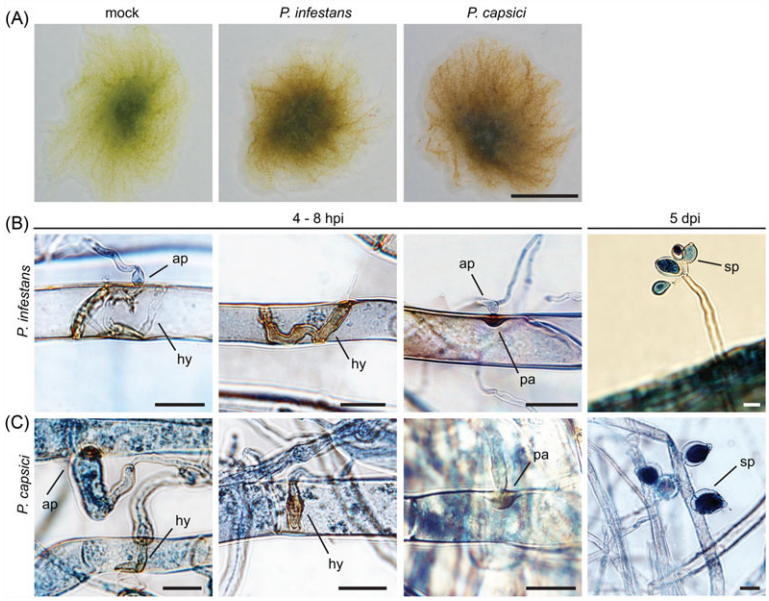

Fig. 2. *P. infestans* and *P. capsici* are able to infect *P. patens*. (A) Moss colonies at 2 dpi with zoospores of *P. infestans* and *P. capsici,* and mock treatment. Scale bar is 5 mm. (B, C) The interaction between *P. patens* and *P. infestans* (B) or *P. capsici* (C) at 4–8 hpi and 5 dpi. The tissue was stained with trypan blue and visualised by brightfield microscopy. Scale bars represent 20 μm. ap, appresorium; hy, intracellular hypha; pa, papilla-like structure; sp, sporangium.

(Figs. 2B and C). Compared to *P. infestans, P. capsici* grew faster and showed more penetration attempts even with similar amounts of zoospores in the inoculum. The intracellular growing hyphae often showed a dark brown coloration. Brown deposits surrounding penetrating hyphae have also been observed during the interaction of *P. infestans* with the nonhost plant species *Arabidopsis thaliana* (Vleeshouwers *et al.*, 2000) and in another moss, *Funaria hygrometrica*, infected by a fungal pathogen (Martinez-Abaigar *et al.*, 2005; Davey *et al.*, 2009; Davey *et al.*, 2010). This dark brown coloration is reminiscent of the deposition of phenolic compounds, a general defence response observed in higher plants (Vleeshouwers *et al.*, 2000).

Besides successful penetration of moss cells, we also observed the formation of papilla-like structures that blocked hyphal penetration and arrested further pathogen colonization (Figs. 2B and C). In fact, roughly half of the penetration attempts were blocked by these papilla-like structures. Papillae are cell wall depositions that are formed by higher plants as part of the first line of defence against fungal and oomycete pathogens (Schmelzer, 2002; Collinge, 2009). Papillae consist of callose, proteins, phenolic compounds and reactive oxygen species and physically resist hyphal penetration (Collinge, 2009). Papilla-like structures in mosses have been reported before. In *P. patens* they were found upon inoculation with the nonvirulent fungus *Apiospora montangei* (Lehtonen *et al.*, 2012b) and in *Funaria hygrometrica* when challenged with *Atradidymella muscivora* and *Coniochaeta velutina* (Davey *et al.*, 2009; Davey *et al.*, 2010). Lehtonen *et al.* (2012b) showed that the papilla-like structures in *P. patens* can be stained with aniline blue, indicating that they contain glucans.

During a later stage of infection, sporangia were detected (Figs. 2B and C), demonstrating that the disease-cycle of *P. infestans* and *P. capsici* can be completed on *P. patens*. However, we have never observed a typical haustorium and combined with the observed defence responses, for example, the deposition of phenolic compounds and the formation of papilla-like structures, we conclude that the interactions between *P. patens* and either *P. infestans* or *P. capsici* resemble nonhost interactions. We therefore consider this pathosystem useful to study basal plant defence responses upon pathogen attack and in particular at early stages of the interaction. Because *P. capsici* shows a higher infection efficiency than *P. infestans*, *P. capsici* was used to analyse this pathosystem in more depth.

Defence-related genes of P. patens *are upregulated upon* Phytophthora *infection*

The overall defence response is usually accompanied with transcriptional reprogramming of defence-related genes (Dodds & Rathjen, 2010). To investigate if this is also the case in the *P. patens – Phytophthora* pathosystem, we studied the expression of six *P. patens* defence-related genes upon *P. capsici* infection, that is, PAL4, LOX7, NOX, MPK4, CHS and ERF5. One-week-old protonema cultures were inoculated with zoospores of *P. capsici* and total RNA was isolated 12 h later. Transcript levels were analysed by qRT-PCR and normalised to their levels in mock-treated protonema cells (Fig. 3). The transcript levels of all studied genes increased upon infection, ranging from 8 up to 58 fold. This indicates that some of the common defence pathways of higher plants are also activated

© 2016 The Authors

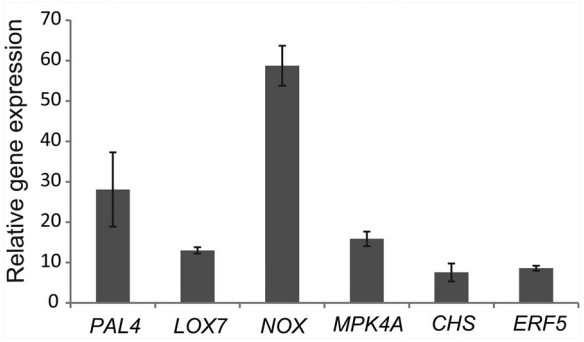

Fig. 3. Defence-related genes are upregulated upon *P. capsici* infection. Transcript levels of six defence-related *P. patens* genes at 12 hpi were analysed by qRT-PCR and normalized to the endogenous *P. patens* gene *EF1α*. The *y*-axis shows the mean fold changes (± standard deviation of 3 technical replicas) relative to the transcript level in moss tissue 12 h after mock treatment that was set at 0. This experiment was repeated at least three times with comparable outcomes.

in *P. patens* upon infection with *Phytophthora*. This is in line with findings in earlier studies dealing with *P. patens* infected with *Botrytis*, *Pythium* or *Colletotrichum* or treated with chitosan (Oliver *et al.*, 2009; Bressendorff, 2012; Ponce de Léon *et al.*, 2012; Lehtonen *et al.*, 2012a; Reboledo *et al.*, 2015).

A set-up for live-cell imaging of moss–pathogen interactions

For high-resolution live-cell imaging of moss cells during pathogen attack, we developed a special set-up that allowed us to image the *Phytophthora–Physcomitrella* interaction over a relatively long time frame (Fig. 4). In this set-up we used prefabricated glass-bottom microwell dishes containing a coverglass as bottom. A moss explant was placed on the glass bottom of the dish, covered with a thin layer of BCD agar and allowed to grow for 5–7 days. In this way, the protonemal tissue grows close to the coverglass and can be maintained in optimal conditions for several days. Most importantly, the glass-bottom microwell dish can be placed directly on the stage of a microscope, so for imaging, the protonema does not have to be disrupted for transfer to a microscope slide. The protonema was inoculated by pipetting a 20 μL droplet of inoculum containing in total 2×10^4 zoospores on top of the thin agar layer. After incubation for at least 4 h in the light, the dish was placed on the stage of an inverted microscope for microscopic analysis. Zoospores germinated and hyphae grew through the thin layer of agar on top of the moss tissue. Pipetting zoospores beneath the thin agar layer by pressing the pipette tip against the coverglass yielded even more penetration attempts.

We have tried several imaging set-ups, but the one we describe here was most effective for imaging *Physcomitrella-Phytophthora* interactions. This method proved the most effective, as the moss tissue did not have to be transplanted between infection and observation. The delicate protonema cells are easily stressed or even die when transferred and this influences their defence capacity. This was illustrated by the inability of *P. patens* to form papilla-like structures when the moss tissue was lifted and placed on top of *Phytophthora* zoospores.

Live-cell imaging reveals local actin accumulation upon Phytophthora *infection.* To demonstrate the power of this set-up for live-cell imaging of plant defence responses, we studied cytoskeletal reorganisation during infection. To easily visualize the cytoskeleton, we generated a transgenic moss line expressing both LifeAct-GFP, a fluorescent marker that binds to filamentous actin (Riedl *et al.*, 2008), and mCherry-tua1, a fusion protein of α-tubulin and the fluorescent tag mCherry. Lifeact-GFP has been used in *Physcomitrella* previously (Vidali *et al.*, 2009). Because overexpression of Lifeact-GFP is known to cause growth defects (Vidali *et al.*, 2009) and inhibits reorganisation of actin filaments in plants (Van der Honing *et al.*, 2011), we carefully screened transgenic moss lines for abnormalities. The line we used behaved similar to wild-type *P. patens* and showed no abnormal growth behaviour or developmental defects.

As shown in Figure 5, the location of the penetration attempt is easily recognised by the strong auto-fluorescence of papilla-like structures when excited by the 561-nm laser line or, in case of successful penetration, by the deposited material around the invasive hyphae. We often observed accumulation of cytoplasm around the penetration site with the nucleus in close proximity (Fig. 5A). Immediately upon penetration and around the papilla-like structures, we observed a rapid accumulation of actin filaments around the site of attack (Figs. 5A and B), but at later stages, after successful penetration of a moss cell by *P. capsici*, the actin cytoskeleton did no longer accumulate around the infection site (Fig. 5C). Similar responses were observed in higher plants, where cytoplasmic accumulation and nuclear repositioning are regarded as basal defence responses upon hyphal penetration attempts (Gross *et al.*, 1993; Schmelzer, 2002; Takemoto & Hardham, 2004; Koh *et al.*, 2005; Hardham, 2007; Huckelhoven & Panstruga, 2011) and where the actin cytoskeleton was found to be essential for proper basal defence against fungal and oomycete pathogens (Takemoto & Hardham, 2004; Hardham *et al.*, 2007; Schmidt & Panstruga, 2007; Day *et al.*, 2011). It has been shown for example that disrupting the actin cytoskeleton by actin depolymerising drugs leads to an increased susceptibility to pathogen attack (Kobayashi *et al.*, 1997; Kobayashi & Hakuno, 2003; Yun *et al.*, 2003; Jarosch *et al.*, 2005; Miklis *et al.*, 2007). Actin accumulation has been observed during both incompatible and compatible interactions and this accumulation has been hypothesised to facilitate vesicle delivery to the infection site (Gross *et al.*, 1993; Takemoto *et al.*, 2003; Opalski *et al.*, 2005; Takemoto *et al.*, 2006; Humbert *et al.*, 2015). Even treatment with fungal elicitors increased actin abundance through the whole cell (Henty-Ridilla *et al.*, 2013; Henty-Ridilla *et al.*, 2014; Li *et al.*, 2015) and mimicking the

© 2016 The Authors

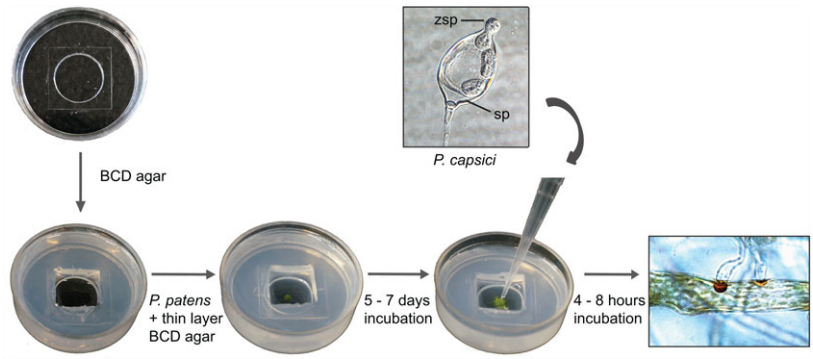

Fig. 4. Set-up for high-resolution live-cell imaging of infected moss cells. A glass-bottom microwell dish (diameter 35 mm) is filled with BCD agar and a square of agar is removed from the middle of the dish. A small explant of *P. patens* is placed in the middle, covered with a thin layer of BCD agar and allowed to grow for 5–7 d. Zoospores (zsp) of *P. capsici* released from sporangia (sp) are used as inoculum. The inoculum is added to the moss tissue by pipetting. After 4 h the first infection attempts can be observed by microscopy.

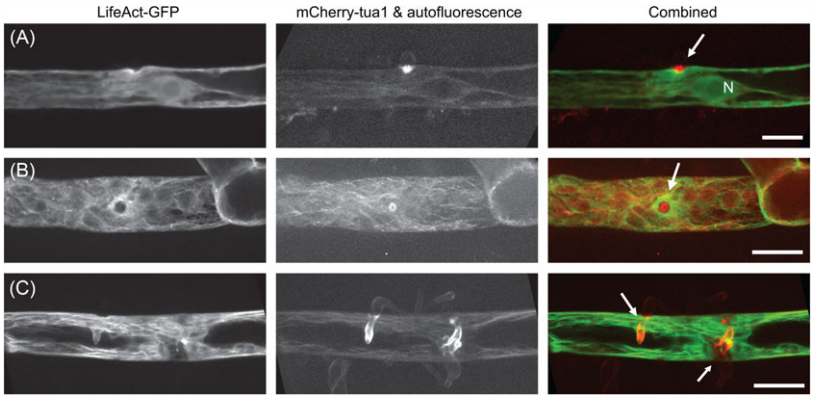

Fig. 5. Subcellular cytoskeleton rearrangements in *P. patens* protonema cells upon *P. capsici* infection. Confocal fluorescent microscopy images of the actin and microtubule cytoskeleton in a transgenic moss line with LifeAct-GFP and mCherry-tua1 at 5 hpi with *P. capsici*. (A) Average Z-projection (1.5 μm) of side view, (B) maximum Z-projection (11 μm) of top view and (C) maximum Z-projection (8.5 μm) of side view. Arrows point to the site of pathogen attack and scale bars represent 10 μm. N, nucleus.

pressure generated by a penetrating pathogen by touching a plant cell with a glass microneedle, resulted in a rapid accumulation of actin at the site of touch (Hardham *et al.*, 2008). This suggests that the changes in actin cytoskeleton that are triggered upon pathogen recognition are both due to molecular cues produced directly or indirectly by the pathogen and due to physical encounter with the pathogen.

In contrast to the actin cytoskeleton, we did not observe a clear change in microtubule organization in *P. patens* upon infection by *Phytophthora* (Fig. 5B). During interphase, cortical microtubules function in guiding cellulose synthase complexes to facilitate cellulose microfibril deposition (Paredez *et al.*, 2006). The behaviour of the microtubule cytoskeleton in response to pathogen infection is variable and its role in plant defence remains unclear (Hardham, 2013). Often, pathogen attack induces depolymerisation of microtubules at the site of attack (Gross *et al.*, 1993; Baluska *et al.*, 1995; Cahill *et al.*, 2002; Takemoto *et al.*, 2003; Takemoto *et al.*, 2006) – a phenomenon that is also observed upon touching with a microneedle (Hardham *et al.*, 2008). Treating plants with microtubule depolymerizing drugs had less effect on defence ability than depolymerizing actin (Hardham, 2013), but did lead to increased susceptibility to a nonhost pathogen in wheat (Li *et al.*, 2010).

Taken together, we showed that cytoplasmic accumulation, nuclear repositioning and actin accumulation upon pathogen penetration are basal subcellular defence processes that were already present in lower plants and that this novel imaging set-up is suitable to visualize subcellular plant defence processes by high-resolution microscopy.

Live-cell imaging of plant–pathogen interactions in perspective

One of the major obstacles for live-cell imaging of plant–pathogen interactions is caused by the fact that often these interactions take place in a subepidermal cell layer of the plant leaf, and this hampers the collection of fluorescent signals by microscopy due to the large working distance and light

© 2016 The Authors

scattering. One way to solve this is by making sections of the infected plant tissue. This was done in a recent live-cell imaging study in which the authors imaged the interaction between *Magnaporthe oryzae* and rice after removing the upper epidermis of the leaf with scissors (Mochizuki *et al.*, 2015). However, this type of manipulation likely induces stress to the plant cells and hence may interfere with a correct interpretation of the observations. A major advantage of *P. patens* is the single-celled nature of the protonema tissue that allows visualization of the plant–pathogen interaction with high-resolution microscopy over time, without the need for manipulation prior to imaging.

Another obstacle is the microscopic visualization of plant proteins. A frequently used approach is transient expression of genes encoding fluorescently-tagged proteins using *Agrobacterium* infiltration and subsequently challenging of the infiltrated leaves with pathogens. The location and behaviour of the tagged proteins in response to pathogen infection can then be monitored by fluorescence microscopy. This approach has, for example, been used for live-cell imaging of proteins involved in endocytic trafficking *Nicotiana benthamiana* and then in particular to monitor their behaviour in response to *P. infestans* infection (Lu *et al.*, 2012). Although this approach is efficient and quickly yields results, it also has serious disadvantages. First of all, agroinfiltration often triggers plant defence responses and that might by itself influence the behaviour of the tagged proteins that are the subject of study. Second, the use of constitutive and strong promoters to drive the expression of genes encoding the fluorescently tagged proteins often leads to overexpression or expression at the wrong time or at the wrong place. This might cause artefacts that change the localization or dynamics leading to wrong interpretations. The advantage of *P. patens* is its convenient toolbox of gene modification. The highly efficient homologous recombination allows direct integration of fluorescent tags in the target gene at the endogenous locus in the genome (Nishiyama *et al.*, 2000). In this way the timing and level of expression of the modified genes is the same as in the wild-type situation and this is especially important when studying proteins that function in a fixed stoichiometry with other proteins or are highly dynamic. The latter certainly applies to subcellular defence response upon pathogen attack.

Outlook

In this study, we developed a novel live-cell imaging set-up to study subcellular defence responses during interactions between the moss *P. patens* and the hemibiotrophic pathogen *Phytophthora*. We used this set-up to visualise the moss cytoskeleton during infection and showed that actin accumulates in *P. patens* around penetration sites, similar to what has been observed in higher plants. In the future, we will use the *Physcomitrella–Phytophthora* pathosystem to study other subcellular defence responses, including exocytosis. This novel pathosytem is also suitable to visualize cellular processes in *Phytophthora* while it is interacting with its host. By using the various fluorescent marker strains of *P. infestans* including LifeAct-GFP transformants (Meijer *et al.*, 2014) we can follow the infection process and the dynamics of the actin cytoskeleton in *Phytophthora* during infection in more detail.

Acknowledgements

We thank Tomohiro Miki from the Goshima lab (Nagoya University, Japan) for kindly providing the *P. patens* mCherry-tua1-HB7 line and Magdalena Bezanilla (University of Massachusetts, USA) for providing the LifeAct-eGFP construct. This research was supported by the Earth and Life Sciences Division and the Technology Foundation of The Netherlands Organization for Scientific Research (PhD grant E. O. and VENI grant K.B., respectively) and by the Wageningen University Fund 'Food-for-Thought campaign'.

References

Akita, M., Lehtonen, M.T., Koponen, H., Marttinen, E.M. & Valkonen, J.P.T. (2011) Infection of the Sunagoke moss panels with fungal pathogens hampers sustainable greening in urban environments. *Sci. Total Environ.* **409**, 3166–3173.

Akita, M. & Valkonen, J.P.T. (2002) A novel gene family in moss (*Physcomitrella patens*) shows sequence homology and a phylogenetic relationship with the TIR-NBS class of plant disease resistance genes. *J. Mol. Evol.* **55**, 595–605.

Andersson, R.A., Akita, M., Pirhonen, M., Gammelgard, E. & Valkonen, J.P.T. (2005) Moss-*Erwinia* pathosystem reveals possible similarities in pathogenesis and pathogen defense in vascular and nonvascular plants. *J. Gen. Plant Pathol.* **71**, 23–28.

Ashton, N.W. & Cove, D.J. (1977) Isolation and preliminary characterization of auxotrophic and analog resistant mutants of moss, *Physcomitrella patens*. *Mol. Gen. Genet.* **154**, 87–95.

Baluska, F., Bacigalova, K., Oud, J.L., Hauskrecht, M. & Kubica, S. (1995) Rapid reorganization of microtubular cytoskeleton accompanies early changes in nuclear ploidy and chromatin structure in postmitotic cells of barley leaves infected with powdery mildew. *Protoplasma.* **185**, 140–151.

Ben Khaled, S., Postma, J. & Robatzek, S. (2015) A moving view: subcellular trafficking processes in pattern recognition receptor-triggered plant immunity. *Ann. Rev. Phytopathol.* **53**, 379–402.

Berriri, S., Garcia, A.V., Frei dit Frey, N. *et al.* (2012) Constitutively active mitogen-activated protein kinase versions reveal functions of *Arabidopsis* MPK4 in pathogen defense signaling. *Plant. Cell.* **24**, 4281–4293.

Bressendorff, S. (2012) Immunity in the moss *Physcomitrella patens*. PhD thesis, University of Copenhagen, Denmark.

Cahill, D., Rookes, J., Michalczyk, A., McDonald, K. & Drake, A. (2002) Microtubule dynamics in compatible and incompatible interactions of soybean hypocotyl cells with *Phytophthora sojae*. *Plant Pathol.* **51**, 629–640.

Caten, C.E. & Jinks, J.L. (1967) Spontaneous variability of single isolates of *Phytophthora infestans*. *Can. J. Bot.* **46**, 329–348.

Collinge, D.B. (2009) Cell wall appositions: the first line of defence. *J. Exp. Bot.* **60**, 351–352.

Cove, D. (2005) The moss *Physcomitrella patens*. *Ann. Rev. Genet.* **39**, 339–358.

© 2016 The Authors

Dao, T.T., Linthorst, H.J. & Verpoorte, R. (2011) Chalcone synthase and its functions in plant resistance. *Phytochem. Rev.* **10**, 397–412.

Davey, M.L. & Currah, R.S. (2006) Interactions between mosses (Bryophyta) and fungi. *Can. J. Bot.* **84**, 1509–1519.

Davey, M.L., Tsuneda, A. & Currah, R.S. (2009) Pathogenesis of bryophyte hosts by the ascomycete *Atradidymella muscivora*. *Am. J. Bot.* **96**, 1274–1280.

Davey, M.L., Tsuneda, A. & Currah, R.S. (2010) Saprobic and parasitic interactions of *Coniochaeta velutina* with mosses. *Botany* **88**, 258–265.

Day, B., Henty, J.L., Porter, K.J. & Staiger, C.J. (2011) The pathogen-actin connection: a platform for defense signaling in plants. *Ann. Rev. Phytopathol.* **49**, 483–506.

Dodds, P.N. & Rathjen, J.P. (2010) Plant immunity: towards an integrated view of plant-pathogen interactions. *Nat. Rev. Genet.* **11**, 539–548.

Donahoo, R.S. & Lamour, K.H. (2008) Interspecific hybridization and apomixis between *Phytophthora capsici* and *Phytophthora tropicalis*. *Mycologia* **100**, 911–920.

Erwin, D.C. & Ribeiro, O.K. (1996) *Phytophthora Diseases Worldwide*, American Phytopathological Society, St. Paul, MN, USA.

Forster, H., Tyler, B.M. & Coffey, M.D. (1994) *Phytophthora sojae* races have arisen by clonal evolution and by rare outcrosses. *Mol. Plant Microbe In.* **7**, 780–791.

Fry, W. (2008) *Phytophthora infestans*: the plant (and R gene) destroyer. *Mol. Plant Pathol.* **9**, 385–402.

Gross, P., Julius, C., Schmelzer, E. & Hahlbrock, K. (1993) Translocation of cytoplasm and nucleus to fungal penetration sites is associated with depolymerization of microtubules and defense gene activation in infected, cultured parsley cells. *EMBO J.* **12**, 1735–1744.

Hardham, A.R. (2001) The cell biology behind *Phytophthora* pathogenicity. *Australas. Plant Path.* **30**, 91–98.

Hardham, A.R. (2007) Cell biology of plant-oomycete interactions. *Cell Microbiol.* **9**, 31–39.

Hardham, A.R. (2013) Microtubules and biotic interactions. *Plant J.* **75**, 278–289.

Hardham, A.R., Jones, D.A. & Takemoto, D. (2007) Cytoskeleton and cell wall function in penetration resistance. *Curr. Opin. Plant Biol.* **10**, 342–348.

Hardham, A.R., Takemoto, D. & White, R.G. (2008) Rapid and dynamic subcellular reorganization following mechanical stimulation of *Arabidopsis* epidermal cells mimics responses to fungal and oomycete attack. *BMC Plant Biol.* **8**, 63.

Henty-Ridilla, J.L., Li, J., Day, B. & Staiger, C.J. (2014) Actin depolymerizing factor 4 regulates actin dynamics during innate immune signaling in *Arabidopsis*. *Plant Cell* **26**, 340–352.

Henty-Ridilla, J.L., Shimono, M., Li, J., Chang, J.H., Day, B. & Staiger, C.J. (2013) The plant actin cytoskeleton responds to signals from microbe-associated molecular patterns. *Plos Pathog.* **9**, e1003290.

Hiwatashi, Y., Obara, M., Sato, Y., Fujita, T., Murata, T. & Hasebe, M. (2008) Kinesins are indispensable for interdigitation of phragmoplast microtubules in the moss *Physcomitrella patens*. *Plant Cell* **20**, 3094–3106.

Huang, J., Gu, M., Lai, Z., Fan, B., Shi, K., Zhou, Y.H., Yu, J.Q. & Chen, Z. (2010) Functional analysis of the *Arabidopsis* PAL gene family in plant growth, development, and response to environmental stress. *Plant physiol.* **153**, 1526–1538.

Huckelhoven, R. & Panstruga, R. (2011) Cell biology of the plant-powdery mildew interaction. *Curr. Opin. Plant Biol.* **14**, 738–746.

Humbert, C., Aimé, S., Alabouvette, C., Steinberg, C. & Olivain, C. (2015) Remodelling of actin cytoskeleton in tomato cells in response to inoculation with a biocontrol strain of *Fusarium oxysporum* in comparison to a pathogenic strain. *Plant Pathol.*

Jarosch, B., Collins, N.C., Zellerhoff, N. & Schaffrath, U. (2005) RAR1, ROR1, and the actin cytoskeleton contribute to basal resistance to *Magnaporthe grisea* in barley. *Mol. Plant Microbe In.* **18**, 397–404.

Judelson, H.S. & Blanco, F.A. (2005) The spores of *Phytophthora*: weapons of the plant destroyer. *Nat. Rev. Microbiol.* **3**, 47–58.

Knight, C., Perroud, P.-F. & Cove, D. (2009) *The Moss Physcomitrella*, Blackwell Publishing, West Sussex, UK.

Kobayashi, I. & Hakuno, H. (2003) Actin-related defense mechanism to reject penetration attempt by a non-pathogen is maintained in tobacco BY-2 cells. *Planta* **217**, 340–345.

Kobayashi, Y., Yamada, M., Kobayashi, I. & Kunoh, H. (1997) Actin microfilaments are required for the expression of nonhost resistance in higher plants. *Plant Cell Physiol.* **38**, 725–733.

Koh, S., Andre, A., Edwards, H., Ehrhardt, D. & Somerville, S. (2005) *Arabidopsis thaliana* subcellular responses to compatible *Erysiphe cichoracearum* infections. *Plant J.* **44**, 516–529.

Kroon, L.P., Brouwer, H., de Cock, A.W. & Govers, F. (2012) The genus *Phytophthora* anno 2012. *Phytopathology* **102**, 348–364.

Lamour, K.H., Stam, R., Jupe, J. & Huitema, E. (2012) The oomycete broad-host-range pathogen *Phytophthora capsici*. *Mol. Plant Pathol.* **13**, 329–337.

Le Bail, A., Scholz, S. & Kost, B. (2013) Evaluation of reference genes for RT qPCR analyses of structure-specific and hormone regulated gene expression in *Physcomitrella patens* gametophytes. *PloS One* **8**, e70998.

Lehtonen, M.T., Akita, M., Frank, W., Reski, R. & Valkonen, J.P. (2012a) Involvement of a class III peroxidase and the mitochondrial protein TSPO in oxidative burst upon treatment of moss plants with a fungal elicitor. *Mol. Plant Microbe In.* **25**, 363–371.

Lehtonen, M.T., Akita, M., Kalkkinen, N., Ahola-Iivarinen, E., Ronnholm, G., Somervuo, P., Thelander, M. & Valkonen, J.P. (2009) Quickly-released peroxidase of moss in defense against fungal invaders. *New Phytol.* **183**, 432–443.

Lehtonen, M.T., Marttinen, E.M., Akita, M. & Valkonen, J.P.T. (2012b) Fungi infecting cultivated moss can also cause diseases in crop plants. *Ann. Appl. Biol.* **160**, 298–307.

Lehtonen, M.T., Takikawa, Y., Ronnholm, G. *et al.* (2014) Protein secretome of moss plants (*Physcomitrella patens*) with emphasis on changes induced by a fungal elicitor. *J. Proteome Res.* **13**, 447–459.

Li, H.L., Wang, H.Y., Hao, X.Y., Song, X.H. & Ma, Q. (2010) Effects of microtubule polymerization inhibitor on the hypersensitive response of wheat induced by the non-host pathogen *Sphaerotheca fuliginea*. *Agric. Sci. China* **9**, 378–382.

Li, J., Henty-Ridilla, J.L., Staiger, B.H., Day, B. & Staiger, C.J. (2015) Capping protein integrates multiple MAMP signalling pathways to modulate actin dynamics during plant innate immunity. *Nat. Commun.* **6**, 7206.

Lu, Y.J., Schornack, S., Spallek, T. *et al.* (2012) Patterns of plant subcellular responses to successful oomycete infections reveal differences in host cell reprogramming and endocytic trafficking. *Cell. Microbiol.* **14**, 682–697.

Martinez-Abaigar, J., Nunez-Olivera, E., Matcham, H.W. & Duckett, J.G. (2005) Interactions between parasitic fungi and mosses: pegged and swollen-tipped rhizoids in *Funaria* and *Bryum*. *J. Bryol.* **27**, 47–53.

© 2016 The Authors

McElroy, D., Zhang, W., Cao, J. & Wu, R. (1990) Isolation of an efficient actin promoter for use in rice transformation. *Plant Cell* **2**, 163–171.

Meijer, H.J., Hua, C., Kots, K., Ketelaar, T. & Govers, F. (2014) Actin dynamics in *Phytophthora infestans*; rapidly reorganizing cables and immobile, long-lived plaques. *Cell. Microbiol.* **16**, 948–961.

Miklis, M., Consonni, C., Bhat, R.A., Lipka, V., Schulze-Lefert, P. & Panstruga, R. (2007) Barley MLO modulates actin-dependent and actin-independent antifungal defense pathways at the cell periphery. *Plant Physiol.* **144**, 1132–1143.

Mochizuki, S., Minami, E. & Nishizawa, Y. (2015) Live-cell imaging of rice cytological changes reveals the importance of host vacuole maintenance for biotrophic invasion by blast fungus, *Magnaporthe oryzae*. *Microbiology Open* **4**, 952–966.

Nishiyama, T., Hiwatashi, Y., Sakakibara, I., Kato, M. & Hasebe, M. (2000) Tagged mutagenesis and gene-trap in the moss, *Physcomitrella patens* by shuttle mutagenesis. *DNA Res.* **7**, 9–17.

Oliver, J.P., Castro, A., Gaggero, C., Cascón, T., Schmelz, E., Castresana, C. & Ponce de León, I. (2009) *Pythium* infection activates conserved plant defense responses in mosses. *Planta* **230**, 569–579.

Opalski, K.S., Schultheiss, H., Kogel, K.H. & Huckelhoven, R. (2005) The receptor-like MLO protein and the RAC/ROP family G-protein RACB modulate actin reorganization in barley attacked by the biotrophic powdery mildew fungus *Blumeria graminis* f.sp *hordei*. *Plant J.* **41**, 291–303.

Paredez, A.R., Somerville, C.R. & Ehrhardt, D.W. (2006) Visualization of cellulose synthase demonstrates functional association with microtubules. *Science* **312**, 1491–1495.

Ponce de León, I. (2011) The moss *Physcomitrella patens* as a model system to study interactions between plants and phytopathogenic fungi and oomycetes. *J Pathog.* 2011: 719873.

Ponce de León, I. & Montesano, M. (2013) Activation of defense mechanisms against pathogens in mosses and flowering plants. *Int. J. Mol. Sci.* **14**, 3178–3200.

Ponce de Léon, I., Oliver, J.P., Castro, A., Gaggero, C., Bentancor, M. & Vidal, S. (2007) *Erwinia carotovora* elicitors and *Botrytis cinerea* activate defense responses in *Physcomitrella patens*. *BMC Plant Biol.* **7**, 52.

Ponce de Léon, I., Schmelz, E.A., Gaggero, C., Castro, A., Alvarez, A. & Montesano, M. (2012) *Physcomitrella patens* activates reinforcement of the cell wall, programmed cell death and accumulation of evolutionary conserved defence signals, such as salicylic acid and 12-oxo-phytodienoic acid, but not jasmonic acid, upon *Botrytis cinerea* infection. *Mol. Plant Pathol.* **13**, 960–974.

Porta, H. & Rocha-Sosa, M. (2002) Plant lipoxygenases. Physiological and molecular features. *Plant Physiol.* **130**, 15–21.

Reboledo, G., Del Campo, R., Alvarez, A., Montesano, M., Mara, H. & Ponce de Léon, I. (2015) *Physcomitrella patens* activates defense responses against the pathogen *Colletotrichum gloeosporioides*. *Int. J. Mol. Sci.* **16**, 22280–22298.

Riedl, J., Crevenna, A.H., Kessenbrock, K. *et al.* (2008) Lifeact: a versatile marker to visualize F-actin. *Nat. Meth.* **5**, 605–607.

Robatzek, S. (2007) Vesicle trafficking in plant immune responses. *Cell. Microbiol.* **9**, 1–8.

Sagi, M. & Fluhr, R. (2006) Production of reactive oxygen species by plant NADPH oxidases. *Plant Physiol.* **141**, 336–340.

Schmelzer, E. (2002) Cell polarization, a crucial process in fungal defence. *Trends Plant Sci.* **7**, 411–415.

Schmidt, S.M. & Panstruga, R. (2007) Cytoskeleton functions in plant-microbe interactions. *Physiol. Mol. Plant P.* **71**, 135–148.

Takemoto, D. & Hardham, A.R. (2004) The cytoskeleton as a regulator and target of biotic interactions in plants. *Plant Physiol.* **136**, 3864–3876.

Takemoto, D., Jones, D.A. & Hardham, A.R. (2003) GFP-tagging of cell components reveals the dynamics of subcellular re-organization in response to infection of *Arabidopsis* by oomycete pathogens. *Plant J.* **33**, 775–792.

Takemoto, D., Jones, D.A. & Hardham, A.R. (2006) Re-organization of the cytoskeleton and endoplasmic reticulum in the *Arabidopsis* pen1-1 mutant inoculated with the non-adapted powdery mildew pathogen, *Blumeria graminis* f. sp. *hordei*. *Mol. Plant Pathol.* **7**, 553–563.

Takikawa, Y., Kida, S., Asayama, F., Nonomura, T., Matsuda, Y., Kakutani, K. & Toyoda, H. (2015) Defence responses of *Aphanoregma patens* (Hedw.) Lindb. to inoculation with *Pythium aphanidermatum*. *J. Bryol.* **37**, 1–7.

Tanigaki, Y., Ito, K., Obuchi, Y. *et al.* (2014) *Physcomitrella patens* has kinase-LRR R gene homologs and interacting proteins. *PloS one* **9**, e95118.

van der Honing, H.S., van Bezouwen, L.S., Emons, A.M. & Ketelaar, T. (2011) High expression of Lifeact in *Arabidopsis thaliana* reduces dynamic reorganization of actin filaments but does not affect plant development. *Cytoskeleton* **68**, 578–587.

van Ooijen, G., van den Burg, H.A., Cornelissen, B.J. & Takken, F.L. (2007) Structure and function of resistance proteins in solanaceous plants. *Ann. Rev. Phytopathol.* **45**, 43–72.

Vidali, L., Rounds, C.M., Hepler, P.K. & Bezanilla, M. (2009) Lifeact-mEGFP reveals a dynamic apical F-actin network in tip growing plant cells. *PloS One* **4**, e5744.

Vijn, I. & Govers, F. (2003) *Agrobacterium tumefaciens* mediated transformation of the oomycete plant pathogen *Phytophthora infestans*. *Mol. Plant Pathol.* **4**, 459–467.

Vleeshouwers, V.G., van Dooijeweert, W., Govers, F., Kamoun, S. & Colon, L.T. (2000) The hypersensitive response is associated with host and nonhost resistance to *Phytophthora infestans*. *Planta* **210**, 853–864.

Wilson, U.E. & Coffey, M.D. (1980) Cytological evaluation of general resistance to *Phytophthora infestans* in potato foliage. *Ann. Bot.* **45**, 81–90.

Xue, J.-Y., Wang, Y., Wu, P., Wang, Q., Yang, L.-T., Pan, X.-H., Wang, B. & Chen, J.-Q. (2012) A primary survey on bryophyte species reveals two novel classes of nucleotide-binding site (NBS) genes. *PloS One* **7**, e36700.

Yun, B.W., Atkinson, H.A., Gaborit, C., Greenland, A., Read, N.D., Pallas, J.A. & Loake, G. J. (2003) Loss of actin cytoskeletal function and EDS1 activity, in combination, severely compromises non-host resistance in *Arabidopsis* against wheat powdery mildew. *Plant J.* **34**, 768–777.

© 2016 The Authors